CRYOSPHERIC SCIENCE NEWS

News date: 4th Nov., 2015 compiled by Dr. Alvarinho J. Luis

The Greenland ice sheet contains nutrients from precipitation

Source: University of Copenhagen - Niels Bohr Institute

Summary: The ice sheet on Greenland contains the nutrient phosphorus, which was carried by the atmosphere and fell with precipitation, new research shows. This new knowledge is important for understanding how many nutrients can be expected to flow into the Arctic Ocean when the climate warms and the ice melts and flows into the sea, where nutrients give rise to increased algae growth.

New research shows that the ice sheet on Greenland contains the nutrient phosphorus, which was carried by the atmosphere across the country, where it fell with precipitation. Studies of the ice core drilling through kilometers-thick ice sheet show that there are differences in the amount of phosphorus in warm and cold climate periods. This new knowledge is important for understanding how many nutrients can be expected to flow into the Arctic Ocean when the climate warms and the ice melts and flows into the sea, where nutrients give rise to increased algae growth. The results have been published in the *J. Geophys. Research (pdf at the end)*.

Phosphorus is an essential nutrient for plant growth in nature and as a fertilizer for food production. 30% of all biological systems rely on phosphorus and nitrate. Nutrients that are not taken up by plants can get washed out into streams and further into the ocean. In addition, phosphorus from the atmosphere is carried to the deep seas, far from land, in the form of precipitation with dust particles. When the sun heats the ocean, some of the water evaporates and rises up into the atmosphere, forming clouds. The clouds can reach an altitude of up to 15 kms and they disperse across the entire globe.

Precipitation and dust storms

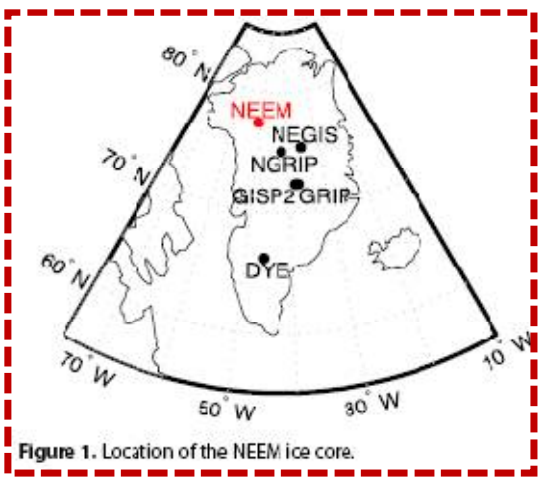

Figure 1. Location of the NEEM ice core.

When the clouds fall as precipitation, it also contains some of the substances, for example, the phosphorus that was in the ocean and this can be measured in the ice cores that are drilled through the more than 2½ kilometers thick ice sheet at the (North Greenland Eemian Ice Drilling Project (NEEM, 77.45°N, 51.06°W) in northwestern Greenland. Because the ice is formed by the snow that falls year after year and remains and is gradually compressed into ice, you can get information about past climate and the nutrient content of the precipitation

But the oceans are not the only contributors of phosphorus. On Earth, there are sometimes great storms that blow dust from dry areas up into the atmosphere, where it spreads across the globe and falls, including on Greenland. The dust also contains phosphorus. Everything that comes down from the atmosphere can be measured in the ice cores.

These researchers have analyzed the ice from different periods between the ice age and the present, to look for total content of phosphorus (total P was determined discretely using an inductively coupled plasma sector field mass spectrometer) and how much of the phosphorus is present in the form of PO_4^{3-}, which is biologically soluble. Both, the amount of P and the ratio between the two variants, P and PO_4^{3-}, help infer the atmospheric transport of nutrients.

Most phosphorus in cold periods

The last ice age lasted about 100 Kyears and ended about 12 Kyears ago, but there were great variations in temperature during the ice age. The analyses show that the amount of phosphorus was greatest during the glacial maximum about 25 Kyears ago and these researchers discovered similarly high levels in other cold periods, while the warm periods during the ice age had 10 times lower the content of phosphorus.

Much of the phosphorus we find in the cold periods is linked to the dust that comes in from the large dust storms. We can see this because it primarily involves the form of phosphate that is not as biodegradable, explains Helle Astrid Kjær, the principal author of the paper.

But they can also see that when there are large volcanic eruptions spewing tons of ash and sulphur far up into the atmosphere, then the atmosphere becomes more acidic and then the phosphorus dissolves into the dust from the dust storms and becomes more soluble and thus more biologically available. This could be seen, for example, in connection with the large Icelandic Laki eruption in 1783 and in 1816 with the Tambora eruption in Indonesia.

Measurements from the period 1770-1820 also show phosphorus, but with a higher ratio of $\mathbf{PO_4^{3-}}$ which is biodegradable. The phosphate is bound together with particles in the atmosphere from large forest fires, while the phosphorus comes from dust.

Measurements from 1930-2004, on the other hand, do not show large amounts of phosphorus and phosphate and this is very surprising, because we use a lot of manure and burn refuse, which can result in large amounts of phosphorus in nature, but it evidently has not reached northern Greenland in precipitation, explains Helle Astrid Kjær.

The nutrient content of the ice is important in a time when we are facing global warming that could mean that large parts of the Greenland ice sheet will melt and flow into the sea. Large amounts of nutrients could lead to an increased growth of algae in the Arctic Ocean.

The amounts of phosphorus and phosphate we have measured are not high compared to the level we normally see in the ocean, but because the ice primarily melts in the spring and summer when the algae are growing and have already used much of the nutrients in the surface water, the level of melt water could lead to an increased growth of algae in the Arctic Ocean, says Helle Astrid Kjær.

pdf reprint follows.....

AGU PUBLICATIONS

JGR

Journal of Geophysical Research: Atmospheres

RESEARCH ARTICLE
10.1002/2015JD023559

Key Points:
- Phosphorus and phosphate concentrations in glacial ice were measured
- Large changes between Holocene and glacial atmospheric transport of P was found
- Large changes in the soluble fraction of P over time was observed

Supporting Information:
- Figures S1 and S2

Correspondence to:
H. A. Kjær,
hellek@fys.ku.dk

Citation:
Kjær, H. A., R. Dallmayr, J. Gabrieli, K. Goto-Azuma, M. Hirabayashi, A. Svensson, and P. Vallelonga (2015), Greenland ice cores constrain glacial atmospheric fluxes of phosphorus, *J. Geophys. Res. Atmos.*, *120*, doi:10.1002/2015JD023559.

Received 22 APR 2015
Accepted 2 OCT 2015
Accepted article online 5 OCT 2015

Greenland ice cores constrain glacial atmospheric fluxes of phosphorus

Helle Astrid Kjær[1], Remi Dallmayr[2], Jacopo Gabrieli[3], Kumiko Goto-Azuma[2,4], Motohiro Hirabayashi[2], Anders Svensson[1], and Paul Vallelonga[1]

[1]Center for Ice and Climate, Niels Bohr Institute, University of Copenhagen, Copenhagen, Denmark, [2]National Institute of Polar Research, Tokyo, Japan, [3]Institute for Dynamics of Environmental Processes, IDPA-CNR, Venice, Italy, [4]Department of Polar Science, The Graduate University for Advanced Studies (SOKENDAI), Tokyo, Japan

Abstract Phosphorus is a limiting nutrient for primary productivity, but little is known about past atmospheric fluxes to the open ocean. In this study, phosphate and phosphorus concentrations have been determined in the North Greenland Eemian Ice Drilling Project ice core for selected periods during the last glacial. Phosphate was determined continuously by using a molybdenum blue spectroscopic absorption method and discretely using an ion chromatograph. Total P was determined discretely using an inductively coupled plasma sector field mass spectrometer. For the last glacial period, we found concentrations of between 3 and 62 nM PO_4^{3-} and 7 and 929 nM P. We find glacial atmospheric fluxes of phosphorus to Greenland were 4 to 11 times higher than in the past century, with the highest input during the cold glacial stadials (GS). Changes in P and PO_4^{3-} fluxes between mild glacial interstadials (GI) and GS correlate positively with dust variability. The soluble fraction of P is larger in the mild GIs as compared to the dust-rich GSs. For the very high phosphate and phosphorus loads during the Last Glacial Maximum, the relationship between phosphate and dust is weaker than in GIs and milder GSs, suggesting either secondary phosphate sources or multiple dust sources. Based on crustal abundances, we find that dust inputs are sufficient to account for all P deposited during all periods investigated except the Last Glacial Maximum. During the glacial, sea salts contributed 10^{-3} nM P, while land biogenic emissions were a minor source of P.

1. Introduction

Phosphorus is an important nutrient for the biosphere and is believed to have been the limiting nutrient for ocean primary productivity in the past [*Falkowski et al.*, 1998] either directly or through its effect on nitrogen fixation [*Okin et al.*, 2011]. Thus, knowing the P load to the ocean is essential in estimating primary productivity [*Redfield*, 1958; *Lenton and Watson*, 2000] and CO_2 drawdown. The atmospheric transport of P to the oceans is small compared to the total P budget of the ocean; however, concentrations of nutrients are often heavily depleted in the surface ocean due to uptake by primary production. For example, colimitation by P and light, especially in the spring and summer seasons, is found for northern Pacific waters and Northwest Atlantic waters [*Arteaga et al.*, 2014]. In sections of the remote ocean where nutrients are not resupplied by upwelling or rivers, atmospheric transport is an especially important source of nutrients to the surface [*Mahowald et al.*, 2008; *Tipping et al.*, 2014].

The oceans are not the only biological systems dependent on P. In a review, it was found that although N limitation is stronger in marine systems, N and P are of equal importance in terrestrial and freshwater systems and that there is a strong synergistic effect in all systems [*Elser et al.*, 2007]. A similar but more recent review found that 28% of the experiments were colimited by P and N, and with similar effects of N and P across systems including marine habitats [*Harpole et al.*, 2011]. Although most terrestrial systems receive their nutrient supply from water flow or from the soil, old forests are believed to be equally limited by phosphorus from atmospheric transport and from water sources as the soil becomes depleted of nutrients over time [*Vitousek and Farrington*, 1997; *Vitousek et al.*, 2010; *Menge et al.*, 2012].

Little is known about the atmospheric deposition of phosphorus, with estimates of atmospheric global P deposition ranging from 0.54 Tg/yr to 3.2 Tg/yr [*Krishnamurthy et al.*, 2010; *Mahowald et al.*, 2008; *Tipping et al.*, 2014]. Furthermore, many poorly constrained assumptions are invoked in calculating dust-related changes in phosphorus transport: the crustal abundance of P varies from approximately 300 ppm to 1300 ppm, invoking

a large uncertainty in the P content of atmospheric dust [*Okin et al.*, 2011, and references therein]. Additionally, the atmospheric transport of dust to the remote oceans is poorly constrained in models, and present-day dust deposition over the oceans differs from observations by an order of magnitude [*Mahowald et al.*, 2009]. Dust-based estimates of the atmospheric transport of P to the oceans are globally about 0.32 Tg/yr, with 0.13 Tg/yr deposited in the Atlantic ocean, 0.073 Tg/yr in the Indian ocean, 0.067 Tg/yr in the Pacific, and 0.032 Tg/yr in the Southern ocean [*Mahowald et al.*, 2008; *Okin et al.*, 2011]. The sources of atmospheric phosphorus are dominated by mineral dust (82%), but also sea salt, primary biogenic particles, and volcanoes are natural sources of P. Soluble phosphorus is less dominated by dust (48%) due to emissions from primary biogenic particles (38%) [*Mahowald et al.*, 2008; *Okin et al.*, 2011].

Total phosphorus fluxes are furthermore insufficient to constrain the effect of P on the biosphere, due to the importance of solubility, speciation, chemical form (inorganic, organic, or colloidal), and other parameters that control the bioavailability of such nutrients. Although limited information is available, one study found that contemporary atmospheric fluxes of soluble organic P to the oceans range from 20% to 83% (0.35 Tg/yr) of atmospheric total soluble phosphorus [*Kanakidou et al.*, 2012]. Other studies find approximately 16% of the total P deposition to the global oceans to be bioavailable [*Krishnamurthy et al.*, 2010]. A recent compilation by *Tipping et al.* [2014] found that 40% of the total P in atmospheric deposition was soluble P (PO_4^{3-}).

The influence of coastal shelves and complementary nutrients has led to much disagreement regarding the glacial-interglacial changes in oceanic productivity and P availability. The shelf nutrient hypothesis [*Broecker*, 1982; *Filippelli*, 2008] proposes that the lower sea level during glacial periods could have enhanced P transport to the oceans. However, other studies suggest that the effect of the continental shelves on primary production is less important [*Ushie and Matsumoto*, 2012]. Records of paleoproductivity are scarce, and the temporal resolution is often low. For the Pacific ocean, the export production during the glacial as compared to present day has been reported as greater [*Kohfeld et al.*, 2005], equal [*Anderson et al.*, 2008; *Ziegler et al.*, 2008; *Tamburini and Fölimi*, 2009], and lower [*Amo and Minagawa*, 2003; *Paytan et al.*, 2004; *Loubere and Richaud*, 2007; *Zhang et al.*, 2007]. The interpretation is complicated by changes in ocean currents, upwelling zones, position of production zones, and mixing layer depth and by changes in deposition rates of nonorganic material [*Tamburini and Fölimi*, 2009; *Maher et al.*, 2010].

Ice cores provide valuable information on large-scale climate and environmental processes, such as atmospheric transport and source region variability [*Fuhrer et al.*, 1996; *Svensson et al.*, 2000; *Ruth et al.*, 2003; *Fischer et al.*, 2007] as well as detailed process information such as past iron fluxes to the ocean and dust iron solubility changes [*Vallelonga et al.*, 2013; *Hiscock et al.*, 2013; *Spolaor et al.*, 2013], besides the well-recognized records of temperature proxies and greenhouse gases [*EPICA Community Members*, 2004; *NGRIP Members*, 2004]. Aeolian dust transport, which is increased during the glacial cold periods [*Svensson et al.*, 2000; *Ruth et al.*, 2003], is expected to enhance the amount of P available to the biosphere. The observed increase in aeolian dust in ice cores in glacial periods is believed to result from more efficient transport mechanisms and drier source areas [*Ruth et al.*, 2003; *Svensson et al.*, 2000; *Mahowald et al.*, 2005].

Only two studies have reported P or PO_4^{3-} from ice cores. *Kjær et al.* [2013] used a molybdenum blue spectroscopic absorption method to find dissolved reactive phosphorus (DRP) with a mean concentration level of 2.74 nM PO_4^{3-} in a shallow Greenland firn core (Northeast Greenland Ice Stream (NEGIS), 75.38°N, 35.56°W) covering the recent century, and 8.06 nM P was found using inductively coupled plasma sector field mass spectroscopy (ICP-SFMS) in two other Greenland shallow firn cores (D4, 71.4°N, 44°W and basin 9, 65°N, 44.9°W) covering the period since 1950 A.D. [*Edwards et al.*, 2007].

In this study, we constrain the late glacial transport of phosphate and total P to Greenland based on the North Greenland Eemian Ice Drilling Project (NEEM, 77.45°N, 51.06°W, see Figure 1) ice core [*Dahl-Jensen et al.*, 2013]. Total P and phosphate were determined in selected sections of the NEEM ice core using different analytical methods. We provide the first evaluation of atmospheric phosphate solubility during the glacial and changes in the glacial atmospheric fluxes of P in the Northern Hemisphere over the last glacial period. Such results are crucial for enhancing the understanding of P source and deposition changes in the past. Further, this study provides concentration ranges of total P and phosphate in Greenland ice, important to constraining nutrient

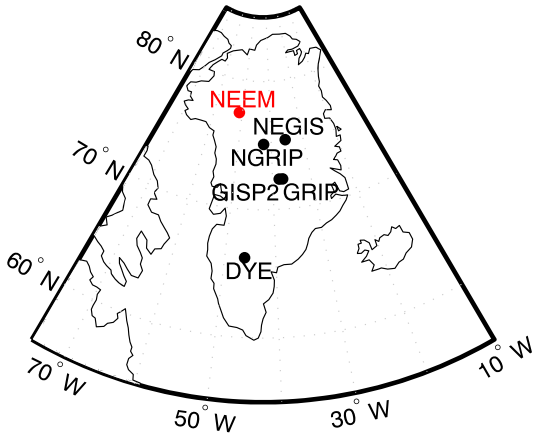

Figure 1. Location of the NEEM ice core.

supply by meltwater and ice discharge from the Greenland ice sheet to the Arctic and North Pacific oceans in a warming world.

2. Methods

In this study, total P and PO_4^{3-} were determined in several glacial sections of the Greenland ice core NEEM by means of four different analytical methods: total P by ICP-MS, PO_4^{3-} by IC, dissolved reactive phosphorus (DRP) by a continuous flow analysis (CFA) molybdenum blue method [*Kjær et al.*, 2013], and acid-labile DRP (DRP_{acid}), which differs from DRP by positioning a particle filter after the addition of molybdenum blue and the buffer as in the discussion paper by *Kjær et al.* [2011]. A summary of the methods are presented in Table 1 and in the supporting information. Ice core sections were drilled in 2009 and sampled in 2010 and 2013/2014. The supporting information contains additional information also on the retrieval and sample procedures.

In 2010, 1.1 m long ice core sections were melted on site in the NEEM camp and determined continuously for DRP_{acid}, the acid-labile fraction of phosphorus, using the DRP technique reported by *Kjær et al.* [2011], which is a modified version of the classical molybdenum blue method. In this method, filtration is performed after addition of molybdenum blue and buffer solution and after several minutes of mixing. Thus, DRP_{acid} is subject to an uncertainty from acid-labile phosphate, which may be leached from particles collected on the filter. Such a leaching causes a shift to higher concentrations until no more leaching takes place or the filter is interchanged.

Several discrete subsamples each integrating 1.1 m of ice were also collected for later analysis. While the continuous measurements were performed at the NEEM field site, the discrete samples were frozen and transported to the National Institute of Polar Research (NIPR) in Japan for determination using IC and to IDPA-CNR, Italy for P detection using ICP-SFMS.

In October–November 2013, replicate continuous DRP measurements were conducted on the NEEM ice core using the recently built continuous-flow analysis system (CFA) at NIPR, Tokyo, Japan [*Kjær et al.*, 2013]. Discrete samples were also collected from the CFA system with a sampling resolution of 5 to 9 cm. These discrete samples were later analyzed for phosphate concentrations by IC and total phosphorus by ICP-SFMS in the same manner as the discrete samples collected in 2010.

The determined concentrations were converted to fluxes for each section of ice investigated by dividing the concentration by the years covered in the section. A discussion of the dating of the NEEM ice core can be found in *Rasmussen et al.* [2013].

Table 1. Analytical Methods Used in This Study

Label	Compound Determined	Concentration Given	Detection Method	Sample Type	Laboratory	Collection Year	Detection Year	LOD	References
A1		P	ICP-SFMS	discrete	IDPA-CNR, Italy	2010	2014	1.6 nM P (50 ppt)	
A2	total P	P		discrete	IDPA-CNR, Italy	2013	2014	1.6 nM P (50 ppt)	
B1	acid-labile P	PO_4^{3-}	DRP_{acid}	continuous	NEEM	2010	2010	1.1 nM PO_4^{3-} (120 ppt)	[*Kjær et al.*, 2011]
C1		PO_4^{3-}	IC	discrete	NIPR, Japan	2010	2011	1.0 nM PO_4^{3-} (110 ppt)	
C2	phosphate	PO_4^{3-}		discrete	NIPR, Japan	2013	2013		
D1	water-labile P	PO_4^{3-}	DRP	continuous	NIPR, Japan	2013	2013	1.1 nM PO_4^{3-} (120 ppt)	[*Kjær et al.*, 2013]

IC, ion chromatograph; LOD, limit of detection; NIPR, National Institute of Polar Research; ppt, parts per thousand.

2.1. Continuous Analysis Methods

Melted NEEM samples were analyzed continuously using a molybdenum blue (MB) reagent determination method. The primary difference between the 2010 and 2013 continuous analyses is the position of a 0.2 μm particle filter, respectively located after and before the point of addition of the MB reagent. The location of the filter after the acidic reagent in the 2010 NEEM continuous-flow analysis (CFA) system allowed acid-labile reactive phosphorus (DRP_{acid}) to be leached from insoluble dust particles [*Kjær et al.*, 2011], whereas the 2013 NIPR CFA setup ensured that only the water-soluble reactive phosphorus (DRP) fraction was determined [*Kjær et al.*, 2013]. The DRP method differs from orthophosphate by the prefiltering of the sample. Due to the use of slower liquid flow rates, the DRP_{acid} system had also a greater dispersion [*Breton et al.*, 2012] of up to 0.5 m and a longer reaction time compared to the 2013 DRP system. This results in lower variability for the results of DRP_{acid} in the NEEM ice core as compared to DRP. The change in resolution is thus due to the system setup rather than a change in deposition rate between the two. Both continuous methods (DRP and DRP_{acid}) were calibrated using PO_4^{3-} standards diluted from a 1 g/L stock solution. The uncertainty of the DRP method is 1.1 nM, resulting from noise on the baseline and uncertainties in the linear fit to standards, which is valid below concentrations of 105 nM PO_4^{3-} [*Kjær et al.*, 2013]. Insoluble dust particle concentrations were also determined continuously using an ABAKUS instrument (Klotz, Germany) [*Bigler et al.*, 2011].

2.2. Discrete Samples

During the 2010 NEEM CFA campaign, discrete samples integrating 1.1 m sections (2 "bags") were collected in precleaned 100 mL polypropylene (As One, Japan) bottles for analysis by ion chromatography (IC) and 10 mL polyethylene (Nalgene Corp., USA) bottles for analysis by ICP-SFMS. These were frozen immediately after collection. Phosphate concentrations were measured by IC in Japan in 2011, and total P was measured by ICP-SFMS in Italy in 2014.

Discrete samples were also collected during the 2013 NIPR CFA campaign using a Gilson FC204 fraction collector kept in a plastic hood supplied with high-efficiency particulate arrestance-filtered air. Each sample integrated either 5 cm if intended for cations only or 9 cm if intended for analysis of both cations and anions. The samples were transferred to polypropylene bottles after each 55 cm "bag" of ice was melted on the CFA system. Immediately after collection, some samples were analyzed by IC, while others were frozen and analyzed within 2 weeks. Some of these discrete samples were also, within 1 week of IC analysis, remelted and reanalyzed in a semidiscrete way for DRP using the molybdenum blue method [*Kjær et al.*, 2013]. Of these, 10 samples from GS2.1, GS8, and GI7 were kept frozen between measurements; 10 from GS5, GI5, and GI7 were kept melted throughout; 2 from GS2.2 (top part) were frozen prior to IC analysis and then kept melted until they were redetected by DRP measurements; and 2 from GS2.2 were kept melted prior to IC detection and then kept frozen prior to DRP reanalysis. After being measured for DRP, all samples were again frozen. In February 2014, the discrete samples collected in 2013 were sent to Venice, Italy, for determination of total P by ICP-SFMS.

Phosphate concentrations were determined discretely at NIPR Japan by a Dionex DX500 ion chromatograph. AS11-HC and CS 14 columns were used for the determination of anions and cations, respectively. No filtering or other pretreatments were applied. For a 5 ppb (52.6 nM) PO_4^{3-} standard, the repeatability of the IC measurements was about 1.5%. The approximate detection limit of the ion chromatograph was 110 ppt (1.0 nM). Blank values (Milli-Q water stored in a similar way to samples) were below the PO_4^{3-} detection limit for the IC.

Total phosphorus concentrations were determined using Thermo Scientific Element 2 inductively coupled plasma sector field mass spectrometry (ICP-SFMS) with an APEX2 (ESI, Omaha, USA) sample introduction system. The samples were not filtered. The recovery of samples ranged from 102% to 108% with a precision of 3–4%. The limit of detection (LOD) for total P was 50 ppt (1.6 nM) P.

2.3. Method Intercomparison

There is no certified reference material available for phosphorus or phosphate in the concentration range or matrix material suitable for polar ice; therefore, we have used diluted phosphate concentration standards (Merck) as a means of intercomparing the methods described here. Phosphate standards used to calibrate the DRP system ranged in concentration from 79 nM to 4.2 nM and were treated similarly to ice samples. The standards were prepared in September 2013 for the NIPR CFA campaign and measured immediately for DRP, and then later for IC (November 2013) and ICP-SFMS (February 2014). The standard concentrations determined by

Table 2. Concentrations, Fluxes, and Solubilities of Phosphorus and Phosphate Observed in the NEEM Glacial Ice[a]

	GS2.1	GS2.2	GS5	GI5	GI7	GS8	Holocene
			Climate Interval				
Age (GICC05) (kyr)	25.17–25.31	25.70–25.84	31.24–31.36	32.27–32.34	35.17–35.24	35.52–35.64	1900–2004 A.D.
Depth (m)—A2, B1, C2, D1	1614.80–1615.90	1619.20–1620.30	1675.85–1676.95	1686.30–1687.40	1718.20–1719.30	1723.70–1724.80	
Depth[b] (m)—A1, C1	1614.15–1616.45	1618.85–1620.85	1675.85–1676.95	1685.75–1687.95	1717.65–1719.85	1723.15–1725.35	
Bag (no.)—A2, B1, C2, D1	2937–2938	2945–2946	3048–3049	3067–3068	3125–3126	3135–3136	
Bag[b] (no.)—A1, C1	2936–2939	2944–2947	3048–3049	3066–3069	3124–3127	3134–3137	
Insoluble particles (# x 10^4/mL)	4.88–28.08	9.58–26.88	3.35–24.40	0.01–6.11	0.15–6.72	2.51–24.22	
			Concentrations				
A1 (nM P)	483–484[b]	340–929[b]	217–225	26–27[b]	22–24[b]	181–189[b]	
A2 (nM P)	248–423	427–637	75–154	17–24	7–17	68–194	8.06
B1 (nM PO_4^{3-})	176–302	284–616	42–108	4–9	5–25	129–300	
C1 (nM PO_4^{3-})	46–62[b]	47[b]	39	12–13[b]	9–10[b]	17–19[b]	
C2 (nM PO_4^{3-})	27–78	27–105	35–51	6–11	4–13	27–45	
D1 (nM PO_4^{3-})	22	32	11	3	4	10	2.74
			Fluxes				
A2 (P nmol yr^{-1} m^{-2})	2.87	4.67	1.09	0.34	0.22	1.31	
B1 (PO_4^{3-} nmol yr^{-1})	2.02	3.40	0.66	0.10	0.24	1.94	
C2 (PO_4^{3-} nmol yr^{-1})	0.50	0.65	0.38	0.14	0.14	0.32	
D1 (PO_4^{3-} nmol yr^{-1})	0.18	0.29	0.10	0.05	0.06	0.09	
			Solubilities				
C2/A2 (%)	18	14	36	41	64	25	
D1/A2 (%)	6	6	9	13	27	7	11–34

[a]The sample ages were determined from the GICC05 timescale [*Rasmussen et al.*, 2013]. The alphanumeric labels refer to the type of measurement applied and sample collection year (see Table 1); as an example, A2 refers to ICP-SFMS analysis on the sample obtained in 2013. Note that results from each detection method was not available for the entire time slice, thus estimates can vary relative to each other due to different temporal sections represented. Also shown are values for the 20th century (Holocene) as observed in other Greenland ice cores [*Edwards et al.*, 2007; *Kjær et al.*, 2013].

[b]Note that, for A1 and C1, often the data represent also the following and previous 0.55 m.

IC were found to be higher than expected with a mean increase of +1.6 nM ± 3.3 nM. For the ICP-SFMS analyses, the difference from the expected concentrations was +1.5 nM ± 2.1 nM (see supporting information). This suggests that some standards were contaminated with P (or PO_4^{3-}) in the process of handling. The level of contamination found is not significant for the results of the glacial stadial samples, but the low concentrations of phosphate found in glacial interstadials are comparable to this level of contamination. This kind of contamination would however only influence discrete samples as, for the continuous DRP method, such a contamination of a standard would be discovered while running the standards and would be removed from the calibration of the sample stream.

3. Results

Table 2 shows the minimum and maximum concentrations of total P determined by ICP-SFMS, DRP_{acid}, and DRP using CFA methods and PO_4^{3-} determined by IC found in the NEEM samples obtained in both 2010 and 2013–2014. These results are also shown in Figure 2 along with insoluble particle concentrations. Note that the discrete samples collected during the 2010 NEEM CFA campaign do not usually correspond to the same depth ranges as those reported for the continuous data or 2013 CFA campaign. The samples collected in 2010 include adjacent 55 cm sections of ice located either above or below those sampled in 2013. As expected, the various phosphate fractions are consistently lower than total phosphorus but vary greatly according to the analytical method used even when performed on exactly the same samples as in 2013. The lowest concentrations were consistently determined by the CFA-DRP technique. Insoluble particle (dust) concentrations follow those observed in other Greenland ice cores [*Ruth et al.*, 2003].

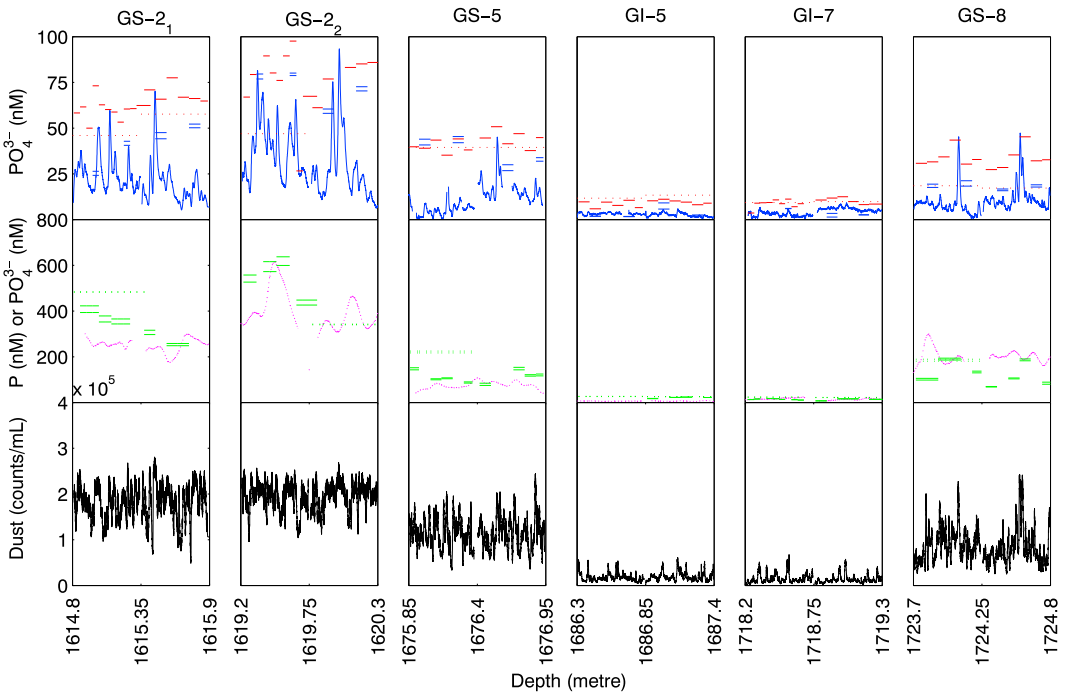

Figure 2. Comparison of phosphorus and phosphate determinations for six climatic periods during the previous glacial. Top: IC-PO_4^{3-} (red) and DRP-PO_4^{3-} (blue). PO_4^{3-} is detected using IC (red); dotted lines represent double bag means (2010 samples), while full lines represent data from 2013; also shown in the top is continuous DRP using CFA (blue) and discrete samples detected using CFA also shown in blue. Middle: ICP-SFMS-P (green) and DRP_{acid}-PO_4^{3-} (magenta). For ICP-SFMS-P, dotted lines represent double bag means (2010 samples), while full lines represent data from 2013. Bottom: Insoluble dust particles (black) as determined using 2013 samples.

4. Discussion

4.1. Comparison of Analytical Methods

Correlations (Table 3) between the different methods of detecting P species in the same samples are high ($r > 0.83$) although the absolute concentrations vary greatly. Usually, the lowest concentrations were determined by CFA-DRP (PO_4^{3-}), with higher IC concentrations (PO_4^{3-}) and even higher DRP_{acid} (PO_4^{3-}). The highest concentrations were consistently found for total P determined by ICP-SFMS. DRP_{acid} concentrations were higher than PO_4^{3-} determined by both IC and DRP methods; the ratios of IC and DRP to DRP_{acid} are 0.53 ± 0.43 and 0.17 ± 0.16, respectively. This is due to the acid reagent in the MB method leaching acid-labile P from insoluble dust particles caught in the filter, thus increasing DRP_{acid} as compared to DRP as discussed in section 2. We find that the ratio of acid-labile phosphorus (DRP_{acid}) to total P is close to 1 (0.96 ± 0.6), suggesting that most of the total P is determined by the DRP_{acid} method. Only for GS-8 is the DRP_{acid} signal consistently greater than total P determined by ICP-SFMS. In this section of the ice core, the DRP_{acid} signal may have been biased to a level greater than that of total P due to the collection of large quantities of acid-labile dust on the filter, as described in section 2.1.

Table 3. Pearson Correlations Between the Different Detections of P and PO_4^{3-} as Well as Correlations to Dust in 5 or 9 cm Resolution Dependent on the Available Discrete Samples[a]

	IC	DRP	ICP-SFMS	DRP_{acid}	Dust
IC	1	0.88	0.90	0.87	0.97
DRP		1	0.94	0.91	0.87
ICP-SFMS			1	0.83	0.90
DRP_{acid}				1	0.93

[a]All P values were $\ll 0.01$. For DRP, IC determined PO_4^{3-} and ICP-MS determined total P; the samples were identical. While for DRP_{acid}, samples were obtained at the same depth, but not strictly identical.

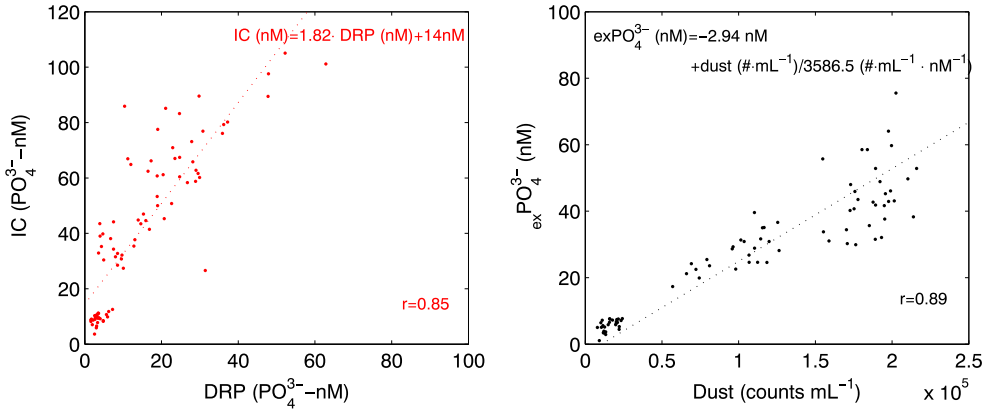

Figure 3. (left) PO_4^{3-} determined using IC against CFA-determined DRP. (right) Difference between DRP and IC-determined PO_4^{3-} as a function of dust. Also shown is the linear fit and Pearson correlations (r). P values are $\ll$0.01.

4.1.1. Effect of Dust on DRP and IC Measurements

A significant deviation between the concentration levels of DRP determined continuously via CFA and PO_4^{3-} detected by IC (a ratio of 0.34±0.14) was also observed. The concentration levels between the two techniques varied by as much as 76 nM, with greater differences for higher concentrations of dust (see Figure 3). The excess PO_4^{3-} determined by IC as compared to the continuous DRP technique correlates linearly with dust (r = 0.89). The relation between the excess phosphate detected by the IC is explained by the IC samples being unfiltered, thus allowing the dust to leach phosphate into the sample, while 0.2 µm particles were filtered from the DRP sample soon after melting (<60 s), thereby quickly removing dust from the sample. Thus, after compensating for the effect of phosphate from soluble dust, the IC values can be corrected to match those detected by DRP. However, the exact fraction of dust-leachable P may depend on the type of dust.

A previous study of DRP determination found that the filtration of surface water samples on 0.2 µm cellulose acetate membranes decreased DRP concentrations by up to 2 nM for sample concentrations ranging from 4.8 to 71 nM [*Patey et al.*, 2010]. The same study found that freezing of unfiltered samples resulted in an increase of approximately 2.7 nM PO_4^{3-}. To investigate if such an effect indeed took place in frozen NEEM samples, a few of the discrete samples collected for IC and total P determination during the 2013 campaign were later determined as discrete samples on the CFA-DRP setup (Figure 2, top graph, blue horizontal lines). For climate periods with high dust loads (glacial stadials), most of the concentrations remeasured were elevated compared to the initial continuous detection of DRP but remained below the concentrations of PO_4^{3-} determined by IC. In contrast, similar concentrations of DRP were found in samples from glacial interstadial periods with low dust concentrations for both discrete and continuous DRP determinations, although the concentration of PO_4^{3-} determined by IC remained consistently higher.

Thus, we find that the PO_4^{3-} concentrations determined by IC exceed those determined by the DRP method for glacial interstadials (warm periods and low dust) samples. This could be due to either the detection limit in the IC technique exceeding the low observations of PO_4^{3-} or the effect of the filter in the DRP method to limit the dissolved P determined by the continuous DRP method. Considering that the limit of detection of the IC method is 1.0 nM and thus well below the determined concentrations even in the glacial interstadials, we conclude that the IC method measures a greater part of the phosphate than the DRP method.

For cold climate periods, the continuous DRP concentrations are low compared to the discrete DRP. This is explained by the limited time available for phosphate to be dissolved from dust between melting and analysis when running continuously, while for the discrete samples, PO_4^{3-} had more time to dissolve. For the cold stadial samples, again the difference between IC and discrete DRP could be explained by the filtering of the DRP-derived PO_4^{3-}.

The same discrete samples as described in section 2.2, remeasured for DRP, were evaluated for effects of handling including freezing and remelting. For the relation between the DRP discrete samples and the IC samples, we do not observe any additional effect of freezing and remelting and the major effect of discrete versus

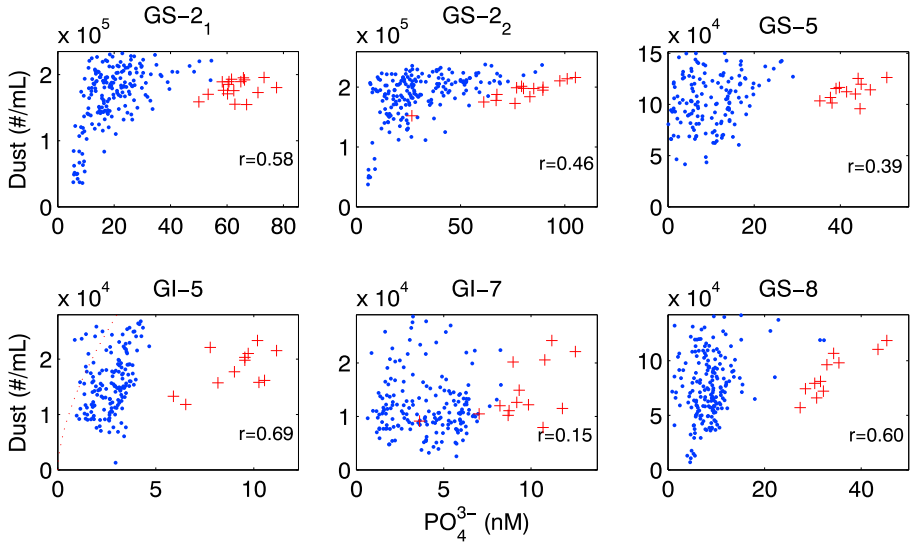

Figure 4. Dust (counts/mL) as a function of PO_4^{3-} for six climatic periods as determined using DRP-CFA (blue) and IC (red). GS denotes glacial stadial and GI glacial interstadial. Numbers indicate Pearson correlation between insoluble dust and DRP in the respective period. All *P* values are better than 0.01, except for GI7 ($P = 0.035$). Please note that the DRP and dust both have been split into 1 cm means for this comparison. Notice the different axes between the plots.

continuous analyses is thus a result of dust leaching in the water phase and filtering of the DRP method and not the IC technique.

4.2. Influence of Climatic Changes on Atmospheric P Deposition

As shown in Table 2 and Figures 2, 4, and 5, significant variability is found in concentrations and fluxes of P and PO_4^{3-} in the NEEM ice core glacial samples. The significant variability at such age and depth suggests that postdepositional effects, which would tend to smooth the signal of P and PO_4^{3-} in ice, are minor.

Phosphate and P concentrations are negatively correlated to temperature proxies δD and $\delta^{18}O$ in the NEEM ice core. In the cold glacial stadials (GS), P and PO_4^{3-} concentrations and fluxes are high. The concentrations determined using CFA-DRP are up to 93 nM PO_4^{3-} in the GS, while the GI has lower concentration between 0.6 nM and 9 nM PO_4^{3-}. The change in PO_4^{3-} concentrations from GI to GS is between a factor of 3 and 12

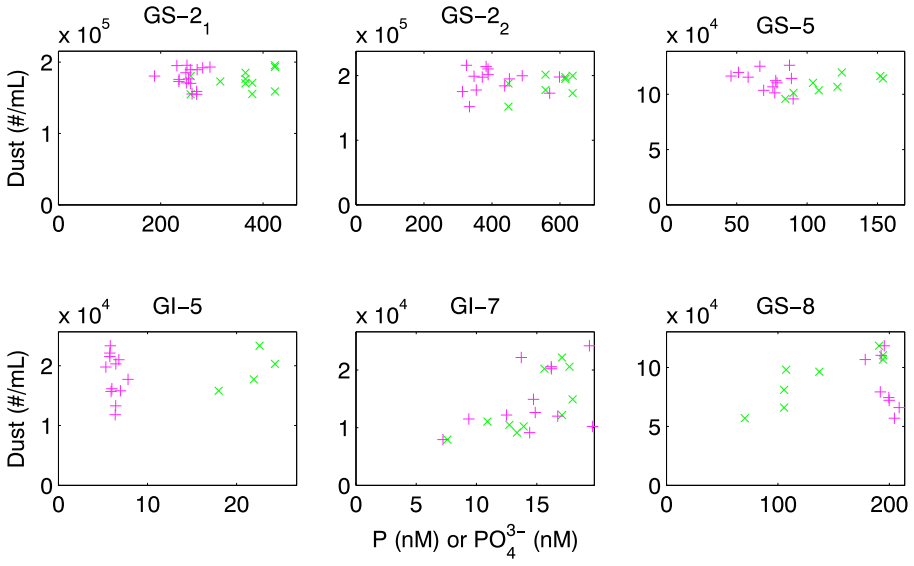

Figure 5. Dust (counts/mL) as a function of PO_4^{3-} or P for six climatic periods as determined using DRP_{acid}-CFA (magenta) and ICP-SFMS (green). GS denotes glacial stadial and GI glacial interstadial.

Table 4. The Rate of Change in Deposition Between Glacial Interstadial (GI) and Glacial Stadials (GS) Shown for the Four Different Methods Used in This Study[a]

	ICP-SFMS Total P		$CFA\text{-}DRP_{acid}$ "Total P"		IC PO_4^{3-}		CFA-DRP PO_4^{3-}	
	Flux	Conc.	Flux	Conc.	Flux	Conc.	Flux	Conc.
GS/GI	3–21	5–39	3–34	5–76	3–5	4–8.8	2–6	3–12
Hol/LGM		~70						~14

[a]Also shown for ICP-SFMS and DRP is the ratio between Holocene estimates found by *Edwards et al.* [2007] and *Kjær et al.* [2013] (Hol), respectively, and Last Glacial Maximum (LGM) represented by $GS2_2$. Note that results from each detection method were not available for the entire time slice; thus, estimates of the ratio can vary relative to each other due to different temporal sections represented.

(fluxes: 1.6 to 6.4), while total P changes by a greater amount, from a factor of 5 to 39 (fluxes: 3.2 to 21, see also Table 4). Similar factors of 15–20 were found for concentrations of dust and dust proxies from GI to GS for other deep Greenland ice cores [*Steffensen*, 1997; *Ruth et al.*, 2003; *Fischer et al.*, 2007; *Maher et al.*, 2010].

Using the only available recent Holocene DRP data from Greenland, the NEGIS firn core (2.74 nM PO_4^{3-}) [*Kjær et al.*, 2013], we find that DRP concentrations during the coldest glacial increased by a factor of 14 (for concentrations, see Table 4), suggesting that the land biosphere is not the main source for PO_4^{3-} found in the Greenland ice. The increase of PO_4^{3-} between the LGM and the Holocene is low compared to that of dust proxies in Greenland, which show concentration decreases of 80 to 100 times from the LGM to the Holocene [*Fischer et al.*, 2007]. The dust in Greenland ice originates from Chinese desert regions, and estimated source changes of a factor of 2–4 have been found in modeling studies, while a 2–12 times increase in transport mechanisms during the glacial is also suggested [*Fischer et al.*, 2007]. If the source region for P is also China, the combination of source and transport changes could account for the 14-fold increase in DRP between the glacial and the Holocene.

4.2.1. Dust

We find that dust is the main source of total P in Greenland ice and that during the LGM, when the fluxes of dust were highest, up to 900 nM P could have originated from dust. While NEEM ice core dust mass concentrations are not yet available, we know from Greenland ice cores with similar accumulation (NEEM 0.22 m/yr), such as the GRIP (0.23 m/yr) and NorthGRIP (0.19 m/yr) ice cores, that approximately 8000–10,000 μg dust/kg ice is found during glacial stadials, while the glacial interstadials show low concentrations on the order of 500 μg/kg [*Svensson et al.*, 2000; *Ruth et al.*, 2003; *Rasmussen et al.*, 2013]. Using the method described by *Kjær et al.* [2013], we assume all dust P is soluble with a mineral dust abundance of 3030 mg/kg. We find that the theoretical upper limit of P present in such dust (P_{dust}) is ~900 nM. This is sufficient to explain total P concentrations observed in the NEEM ice core during the glacial stadials (Figure 5). However, the abundance ratio of P varies in different dust sources with the 3030 mg/kg dust used here in the high end compared to P concentrations in surface soils (700–1300 ppm) [*Mahowald et al.*, 2008], which would yield P concentrations from dust of 220–420 nM P. Thus, using mean crustal values, the derived P_{dust} can explain 40–75% of the 564 nM total P determined by ICP-SFMS. In the warm glacial interstadials, P_{dust} is between 10 and 20 nM P using crustal abundances and ~50 nM using rock dust abundances and thus can explain all of the P found using ICP-SFMS in the NEEM ice. While atmospheric dust compositions can vary significantly from crustal mean abundances depending on the mineral composition of each individual dust particles [*Nenes et al.*, 2011], we find that crustal sources account for at least 40% of P during the glacial stadials and all P during the glacial interstadials.

We also find high correlations between IC-determined dust species (Ca^{2+}, Mg^{2+}, K^+, and F^-) and PO_4^{3-} (IC), while the high-resolution DRP has a lower correlation to continuous determined insoluble dust (Table 3), which could suggest more complicated processes than simple dust transport, such as a rainout effect or secondary sources. The IC PO_4^{3-} concentrations determined in 2013 correlate to other soluble dust species such as Ca^{2+}, Mg^{2+}, K^+, and F^- determined on the same samples by 0.94, 0.95, 0.97, and 0.94 (Pearson correlations, $P < 0.01$), respectively. Though the IC results from NIPR 2013 are of high resolution (5–9 cm ice) compared to many other discrete measurements performed normally on 55 cm ice pieces, correlation analysis of data that do not resolve annual patterns can only be tentatively trusted. We thus find that correlations between PO_4^{3-} and other IC-determined ions such as sea salt-related Na^+ and Cl^- are also high (0.89 and 0.83) and that also the land biogenic species NH_4^+ [*Fuhrer et al.*, 1996] correlates by 0.83. NO_3^- is affected by

postdepositional effects [*Rothlisberger et al.*, 2002] and had a correlation of 0.65 to PO_4^{3-}, and methanesulfonic acid, which is related to the ocean biosphere production [*Jaffrezo et al.*, 1994], did not correlate with PO_4^{3-} ($r = 0.01$, $P > 0.01$).

Although individual high peaks observed in the DRP record generally coincide with peaks in dust (Figure 2) and the P concentrations by ICP-SFMS and PO_4^{3-} (by IC) are strongly related to dust, the high-resolution DRP data show that there is a decoupling of DRP and insoluble dust for high DRP concentrations especially during the Last Glacial Maximum (LGM, GS2). DRP-dust correlations during different climatic periods are shown in Figure 4. The correlations are similar for all glacial stadials (r values from 0.4 to 0.6) but vary greatly between the two interstadials (r values of 0.15 and 0.7). This large variability may be due to a combination of factors such as (1) preweathering differences, for example variations in the acidity of the water in the atmosphere affecting the solubility during transport and/or different atmospheric transport mechanisms, (2) postdepositional changes, e.g., influenced by acid layers in the ice, and (3) finally as discussed below different sources of dust having different soluble fractions of P.

In conclusion, most of the glacial P determined in the NEEM ice core likely originates from dust, but we can not exclude other sources.

4.2.2. Solubility

We find significant variability in the soluble fraction of P in the six different climatic periods (Table 2), which cannot be directly inferred from the dust concentration alone. Similar cases of decoupling between nutrient solubility (such as iron) and dust concentrations have been found in other ice cores [*Vallelonga et al.*, 2013; *Hiscock et al.*, 2013; *Spolaor et al.*, 2013]. The ratios of PO_4^{3-} determined by IC and DRP detection methods to P determined by ICP-SFMS were 38 ± 24 and $13 \pm 13\%$ in the NEEM ice, respectively (Table 2). We find that the soluble fraction of P is two to four times greater during glacial interstadials as compared to glacial stadials. In comparison, *Kjær et al.* [2013] found DRP concentrations of 2.74 nM in the 100 year old strata of the Greenland NEGIS firn core, while *Edwards et al.* [2007] found total P concentrations of 8 nM in another Greenland firn core. While care must be taken when comparing different ice cores, the highest soluble fraction (34%) calculated for late Holocene (postindustrialization) ice when assuming the accumulation is similar for the two shallow cores is greater than the range observed for the glacial. This result is only valid if P and P species are exclusively wet deposited. If P is dry deposited, its solubility would be influenced by the amount of accumulation, in which case the solubility in the recent period is a mere 11% as the accumulation at the site studied by *Kjær et al.* [2013] is about one third of the accumulation of the study site of *Edwards et al.* [2007].

The recent compilation by *Tipping et al.* [2014] including global atmospheric deposition data for recent times finds very similar solubilities (40%) as those found in this study for the postindustrial period (34%) when assuming wet-deposited P [*Edwards et al.*, 2007; *Kjær et al.*, 2013]. It has been found that the amount of soluble reactive phosphorus to total phosphorus varies between 8% and 18% in liquid precipitation for dust sources and up to 98% for marine salts while precipitation originating from biomass burning showed intermediate solubility [*Zamora et al.*, 2013]. Other studies have found solubilities of total inorganic P of up to >80% in cases of acidic emissions to the atmosphere (e.g., volcanic eruptions) [*Nenes et al.*, 2011].

The acidity of the atmosphere is decreased during glacial periods due to high particle loads [*Taylor et al.*, 1993], and higher acidity concentrations are found in GIs as compared to GS periods [*Wolff et al.*, 1997]. This could explain why the soluble fraction of P found in the NEEM ice core is low during the GSs and higher during the GIs. However, other studies show increased volcanic activity in the period around 35 to 22 kyr B.P. [*Zielinski et al.*, 1996]. *Fischer et al.* [1998] reported sulfate and nitrate concentrations in Greenland ice, demonstrating high levels of atmospheric acids especially during the 20th century. This supports the hypothesis that the changing acidity of the atmosphere, especially in recent times, influences the soluble fraction of total P, but it does not discount solubility changes due to source variability and transport processes.

4.2.3. Biosphere

We do not find the land biosphere to be a source of P deposited in polar ice, because P is decreasing during the transition from cold periods to warm periods, while an increase would be expected if P was related to the North American biosphere. Such a transition was found in other land biogenic sources such as ammonium and formate [*Fuhrer et al.*, 1996]. The ammonium signal is generally used as a proxy for the land biosphere [*Fuhrer et al.*, 1996] and is one of the few species that decrease during the cold glacial climate periods, even though higher NH_4^+ concentrations are observed during cold GSs than warm GIs. The trend between Holocene and glacial is explained by the Laurentide ice sheet covering most of North America during the recent glacial period, thus suppressing the biosphere signal, while the trends between GI and GS are explained by transport

changes, with stronger winds in cold periods [*Fuhrer et al.*, 1996]. The change between glacial and interglacial periods is opposite for phosphorus and phosphate; thus, if phosphorus determined in the NEEM ice core has a biogenic land component, it is minor. However, one should be aware that changes in deposition and transport could mask the effect of such a source.

4.2.4. Sea Salt

While sea salt is not a major source of atmospheric P in recent times [*Mahowald et al.*, 2008], the rate of change between concentrations of P in recent times and the observations of P found in the NEEM ice fits the 10–15 times change observed for Na^+ in the Greenland Ice Sheet Project 2 ice core [*Fischer et al.*, 2007]. To investigate whether sea salt is a possible source of P during the glacial, we use Na^+ and Cl^- data from IC and CFA measurements of NEEM ice. Assuming that both ions originate only from sea salt and using the Cl^-/PO_4^{3-} ratio in sea salt, $R^{Cl}_{sea\ salt} = 5.53 \times 10^{-7}$ and $R^{Na}_{sea\ salt} = 8.14 \times 10^{-7}$ [*Gianguzza et al.*, 2002; *Concright et al.*, 2000], we determine the concentration of salt-derived P during the glacial. The high-resolution sea-salt concentrations found using CFA in 2010 vary between 8.7 and 524 ppb Na^+ (0.4–22.8 μM), while the IC data obtained in 2013 vary between 17 and 214 ppb for Na^+ and 36 and 335 ppb for Cl^-. Thus, the sea salt-derived PO_4^{3-} is on the order of 10^{-3} nM (picomolar concentrations), which is insufficient to explain the concentration levels found in the NEEM glacial ice.

4.3. Nutrient Supply From the Greenland Ice Sheet in a Warming World

Given the concentrations of P and PO_4^{3-} found in this study and the annual melt rate of the Greenland ice sheet, we can constrain the P supply from the Greenland ice sheet to the Arctic ocean. According to Gravity Recovery and Climate Experiment satellite estimates, the Greenland ice sheet has lost ~258 of mass annually with significant annual variability varying from 6 Gt/yr (2013–2014) to 474 Gt/yr (2012–2013) [*Velicogna and Wahr*, 2013; *Tedesco et al.*, 2014]. Using the mean rate of Greenland melt and the concentration of P and PO_4^{3-} for the glacial found in this study, the annual amount of P added to the global oceans from the Greenland ice sheet is on the order of 10^8 g P/yr, corresponding to less than 0.1% of that added from the atmosphere to the global oceans or 0.6% of that from the atmosphere to the Atlantic ocean. Using Holocene concentrations, the total released P from the Greenland ice sheet to the oceans is about 100 times less. While the melt from Greenland contributes only small amounts of P, it is important to recall that the melt takes place in spring and summer when the biospheric production increases and that *Arteaga et al.* [2014] found that the waters surrounding Greenland are limited by the availability of P (and light) exactly during the spring and summer months. Thus, P release from from the Greenland ice sheet may be effective on local or regional scales.

5. Conclusion

In this study, P and PO_4^{3-} concentrations have been determined for the first time in Greenland glacial ice. We studied sections covering between 35.6 and 25.2 kyr B.P. and found total P concentrations between 7 and 637 nM (fluxes of 0.22–4.67 nM yr^{-1} m^{-2}), with soluble PO_4^{3-} concentrations between 4 and 62 nM (fluxes of 0.05–0.65 nM yr^{-1} m^{-2}).

We find concentrations of both PO_4^{3-} and P increased by factors of 3–12 and 5–39 during the cold glacial stadials (GS) as compared to the milder glacial interstadials (GI), respectively. For dissolved reactive phosphorus (DRP), a 14-fold change was found between GS-2 and recent concentrations of the past 100 years [*Kjær et al.*, 2013]. Flux change ratios were 3.2–21 for total P, while fluxes of dissolved P varied by 1.6 to 6.4 times between glacial stadials and interstadials.

While the rate of change for P and PO_4^{3-} is lower than that observed for dust, the P concentrations fit those expected from a dust input in the glacial interstadials, while for the Last Glacial Maximum (LGM) the dust-derived P is capable of explaining the load of total P in the NEEM ice (77.45°N, 51.06°W). When using a lower-resolution data set (5–9 cm, IC and ICP-SFMS), we find significant correlation to other dust ions. When using high-resolution continuous measurements of insoluble dust and DRP, the correlation is lower, which could indicate secondary P sources or multiple dust source regions. The level of sea salt-derived P is far lower than the P concentrations found in the NEEM ice, and therefore, sea salts are unlikely to be a significant source.

The mean soluble fraction of P during the period investigated varies from 13% to 38% depending on the detection method used, with higher soluble fractions during the warm interglacial periods. We suggest that the larger solubility during warm interglacial periods could be caused by changes in source regions, by multiple sources, or by an increased acidity in glacial interstadials as compared to glacial stadials due to less carbonates in the atmosphere. However, further studies are needed to distinguish between these effects.

This study shows that the P and PO_4^{3-} concentrations found in the NEEM ice core fit those expected if dust is the main source, while the relative change between GSs and GIs is lower than would be expected from a dust proxy. The variability between dust-derived P and the levels of P and PO_4^{3-} reported here between different periods in the past glacial demonstrates the continued importance of observational data to accurately estimate atmospheric nutrient supply to the oceans in the past. Further, this study shows that relying on dust flux changes to determine atmospheric nutrient deposition does not accurately resolve changes in the P solubility. Finally, the concentrations of both soluble P and total P presented here are crucial to constraining the importance of meltwater and iceberg discharge from Greenland ice as a nutrient source for Arctic waters in the coming future.

Acknowledgments
The data presented are part of the NEEM ice core drilling program. NEEM is directed and organized by the Center of Ice and Climate at the Niels Bohr Institute and US NSF, Office of Polar Programs. It is supported by funding agencies and institutions in Belgium (FNRS-CFB and FWO), Canada (NRCan/GSC), China (CAS), Denmark (FIST), France (IPEV, CNRS/INSU, CEA, and ANR), Germany (AWI), Iceland (RannIs), Japan (NIPR), Korea (KOPRI), the Netherlands (NWO/ALW), Sweden (VR), Switzerland (SNF), UK (NERC), and the USA (US NSF, Office of Polar Programs). The CFA campaign at the National Institute of Polar Research (NIPR) in 2013 was supported by JSPS KAKENHI grant 22221002. Data can be obtained by emailing the lead author using the email address Hellek@fys.ku.dk.

References

Amo, M., and M. Minagawa (2003), Sedimentary record of marine and terrigenous organic matter delivery to the Shatsky rise, western North Pacific, over the last 130 kyr, *Org. Geochem.*, *34*(9), 1299–1312.

Anderson, L. A., and J. L. Sarmiento (1994), Redfield ratios of remineralization determined by nutrient data analysis, *Global Biogeochem. Cycles*, *8*(1), 65–80.

Anderson, R., M. Fleisher, Y. Lao, and G. Winckler (2008), Modern $CaCO_3$ preservation in equatorial Pacific sediments in the context of late-Pleistocene glacial cycles, *Mar. Chem.*, *111*(1), 30–46.

Arteaga, L., M. Pahlow, and A. Oschlies (2014), Global patterns of phytoplankton nutrient and light colimitation inferred from an optimality-based model, *Global Biogeochem. Cycles*, *28*, 648–661, doi:10.1002/2013GB004668.

Bigler, M., A. Svensson, E. Kettner, P. Vallelonga, M. E. Nielsen, and J. P. Steffensen (2011), Optimization of high-resolution continuous flow analysis for transient climate signals in ice cores, *Environ. Sci. Technol.*, *45*(10), 4483–4489, doi:10.1021/es200118j.

Breton, D. J., B. G. Koffman, A. V. Kurbatov, K. J. Kreutz, and G. S. Hamilton (2012), Quantifying signal dispersion in a hybrid ice core melting system, *Environ. Sci. Technol.*, *46*(21), 11,922–11,928.

Broecker, W. S. (1982), Glacial to interglacial changes in ocean chemistry, *Prog. Oceanogr.*, *11*(2), 151–197.

Concright, M. E., W. W. Gregg, and S. Levitus (2000), Seasonal cycle of phosphate in the open ocean, *Deep Sea Res., Part I*, *47*, 159–175.

Dahl-Jensen, D., et al. (2013), Eemian interglacial reconstructed from a Greenland folded ice core, *Nature*, *493*(7433), 489–494.

Edwards, R., J. McConnell, and J. Banta (2007), Atmospheric deposition of iron and phosphorus to Greenland over the 20th-century, *Eos Trans. AGU*, *88*(52), Fall Meet. Suppl., Abstract A53B–1154.

Elser, J. J., C. E. Cleland, D. S. Gruner, W. S. Harpole, J. T. Ngai, E. W. Seabloom, J. B. Shurin, and J. E. Smith (2007), Global analysis of nitrogen and phosphorus limitation of primary producers in freshwater, marine and terrestrial ecosystems, *Ecol. Lett.*, *10*, 1135–1142.

EPICA Community Members (2004), Eight glacial cycles from an Antarctic ice core, *Nature*, *431*, 623–628.

Falkowski, P. G., R. T. Barber, and V. Smetacek (1998), Biogeochemical controls and feedbacks on ocean primary production, *Science*, *281*(5374), 200–206.

Filippelli, G. M. (2008), The global phosphorus cycle: Past, present, and future, *Elements*, *4*, 89–95.

Fischer, H., D. Wagenbach, and J. Kipfstuhl (1998), Sulfate and nitrate firn concentrations on the Greenland ice sheet: 1. Large-scale geographical deposition changes, *J. Geophys. Res.*, *103*(D17), 21,927–21,934.

Fischer, H., M.-L. Siggard-Andersen, U. Ruth, and R. W. E. Röthlisberger (2007), Glacial/interglacial changes in mineral dust and sea-salt records in polar ice cores: Sources, transport, and deposition, *Rev. Geophys.*, *45*, RG1002, doi:10.1029/2005RG000192.

Fuhrer, K., A. Neftel, M. Anklin, T. Staffelbach, and M. Legrand (1996), High-resolution ammonium ice core record covering a complete glacial inter-glacial cycle, *J. Geophys. Res.*, *101*(D2), 4147–4164.

Gianguzza, A., E. Pelizzetti, and S. Sammartano (2002), *Chemistry of Marine Water and Sediments*, 5 pp., Springer, Berlin.

Harpole, W. S., et al. (2011), Nutrient co-limitation of primary producer communities, *Ecol. Lett.*, *14*(9), 852–862.

Hiscock, W. T., H. Fischer, M. Bigler, G. Gfeller, D. Leuenberger, and O. Mini (2013), Continuous flow analysis of labile iron in ice-cores, *Environ. Sci. Technol.*, *47*(9), 4416–4425.

Jaffrezo, J.-L., C. I. Davidson, M. Legrand, and J. E. Dibb (1994), Sulfate and MSA in the air and snow on the Greenland ice sheet, *J. Geophys. Res.*, *99*(D1), 1241–1253.

Kanakidou, M., et al. (2012), Atmospheric fluxes of organic N and P to the global ocean, *Global Biogeochem. Cycles*, *26*, GB3026, doi:10.1029/2011GB004277.

Kjær, H., A. Svensson, P. Vallelonga, E. Kettner, S. Schüpbach, M. Bigler, J. Steffensen, and M. Hansson (2011), First continuous phosphate record from Greenland ice cores, *Clim. Past Discuss.*, *7*(6), 3959–3989.

Kjær, H. A., P. Vallelonga, A. Svensson, M. E. L. Kristensen, C. Tibuleac, and M. Bigler (2013), Continuous flow analysis method for determination of dissolved reactive phosphorus in ice cores, *Environ. Sci. Technol.*, *47*(21), 12,325–12,332.

Kohfeld, K. E., C. Le Quéré, S. P. Harrison, and R. F. Anderson (2005), Role of marine biology in glacial-interglacial CO_2 cycles, *Science*, *308*(5718), 74–78.

Krishnamurthy, A., J. K. Moore, N. Mahowald, C. Luo, and C. S. Zender (2010), Impacts of atmospheric nutrient inputs on marine biogeochemistry, *J. Geophys. Res.*, *115*, G01006, doi:10.1029/2009JG001115.

Lenton, T. M., and A. J. Watson (2000), Redfield revisited: 1. Regulation of nitrate, phosphate, and oxygen in the ocean, *Global Biogeochem. Cycles*, *14*(1), 225–248.

Loubere, P., and M. Richaud (2007), Some reconciliation of glacial-interglacial calcite flux reconstructions for the eastern Equatorial Pacific, *Geochem. Geophys. Geosyst.*, *8*, Q03008, doi:10.1029/2006GC001367.

Maher, B., J. Prospero, D. Mackie, D. Gaiero, P. Hesse, and Y. Balkanski (2010), Global connections between aeolian dust, climate and ocean biogeochemistry at the present day and at the Last Glacial Maximum, *Earth Sci. Rev.*, *99*(1), 61–97.

Mahowald, N., et al. (2008), Global distribution of atmospheric phosphorus sources, concentrations and deposition rates, and anthropogenic impacts, *Global Biogeochem. Cycles*, *22*, GB4026, doi:10.1029/2008GB003240.

Mahowald, N. M., A. R. Baker, G. Bergametti, N. Brooks, R. A. Duce, T. D. Jickells, N. Kubilay, J. M. Prospero, and I. Tegen (2005), Atmospheric global dust cycle and iron inputs to the ocean, *Global Biogeochem. Cycles*, *19*, GB4025, doi:10.1029/2004GB002402.

Mahowald, N. M., et al. (2009), Atmospheric iron deposition: Global distribution, variability, and human perturbations, *Annu. Rev. Mar. Sci.*, *1*, 245–278.

Menge, D. N., L. O. Hedin, and S. W. Pacala (2012), Nitrogen and phosphorus limitation over long-term ecosystem development in terrestrial ecosystems, *PLoS One*, *7*(8), e42045.
Nenes, A., M. D. Krom, N. Mihalopoulos, P. Van Cappellen, Z. Shi, A. Bougiatioti, P. Zarmpas, and B. Herut (2011), Atmospheric acidification of mineral aerosols: A source of bioavailable phosphorus for the oceans, *Atmos. Chem. Phys.*, *11*(13), 6265–6272, doi:10.5194/acp-11-6265-2011.
NGRIP Members (2004), High-resolution record of Northern Hemisphere climate extending into the last interglacial period, *Nature*, *431*, 147–151.
Okin, G. S., et al. (2011), Impacts of atmospheric nutrient deposition on marine productivity: Roles of nitrogen, phosphorus, and iron, *Global Biogeochem. Cycles*, *25*, GB2022, doi:10.1029/2010GB003858.
Patey, M. D., E. P. Achterberg, M. J. Rijkenberg, P. J. Statham, and M. Mowlem (2010), Interferences in the analysis of nanomolar concentrations of nitrate and phosphate in oceanic waters, *Anal. Chim. Acta*, *673*(2), 109–116.
Paytan, A., M. Lyle, A. Mix, and Z. Chase (2004), Climatically driven changes in oceanic processes throughout the equatorial Pacific, *Paleoceanography*, *19*, PA4017, doi:10.1029/2004PA001024.
Rasmussen, S. O., et al. (2013), A first chronology for the North Greenland Eemian ice drilling (NEEM) ice core, *Clim. Past*, *9*(6), 2713–2730.
Redfield, A. C. (1958), The biological control of chemical factors in the environment, *Am. Sci.*, *46*(3), 205–221.
Rothlisberger, R., et al. (2002), Nitrate in Greenland and Antarctic ice cores: A detailed description of post-depositional processes, *Ann. Glaciol.*, *35*(1), 209–216.
Ruth, U., D. Wagenbach, J. P. Steffensen, and M. Bigler (2003), Continuous record of microparticle concentration and size distribution in the central Greenland NGRIP ice core during the last glacial period, *J. Geophys. Res.*, *108*(D3), 4098, doi:10.1029/2002JD002376.
Spolaor, A., P. Vallelonga, J. Gabrieli, M. Roman, and C. Barbante (2013), Continuous flow analysis method for determination of soluble iron and aluminium in ice cores, *Anal. Bioanal.Chem.*, *405*(2–3), 767–774.
Steffensen, J. P. (1997), The size distribution of microparticles from selected segments of the Greenland ice core project ice core representing different climatic periods, *J. Geophys. Res.*, *102*(C12), 26,755–26,763.
Svensson, A., P. E. Biscaye, and F. E. Grousset (2000), Characterization of late glacial continental dust in the Greenland ice core project ice core, *J. Geophys. Res.*, *105*(D4), 4637–4656.
Tamburini, F., and K. Fölimi (2009), Phosphorus burial in the ocean over glacial-interglacial time scales, *Biogeosciences*, *6*(4), 501–513.
Taylor, K., C. Hammer, R. Alley, H. Clausen, D. Dahl-Jensen, A. Gow, N. Gundestrup, J. Kipfstuhl, J. Moore, and E. Waddington (1993), Electrical conductivity measurements from the GISP 2 and GRIP Greenland ice cores, *Nature*, *366*(6455), 549–552.
Tedesco, M., J. Box, J. Cappelen, X. Fettweis, T. Mote, R. van de Wal, C. Smeets, and J. Wahr (2014), Greenland ice sheet. [Available at www.arctic.noaa.gov/reportcard], p. 22.
Tipping, E., et al. (2014), Atmospheric deposition of phosphorus to land and freshwater, *Environ. Sci. Processes Impacts*, *16*, 1608–1617.
Ushie, H., and K. Matsumoto (2012), The role of shelf nutrients on glacial-interglacial CO_2: A negative feedback, *Global Biogeochem. Cycles*, *26*, GB2039, doi:10.1029/2011GB004147.
Vallelonga, P., C. Barbante, G. Cozzi, J. Gabrieli, S. Schüpbach, A. Spolaor, and C. Turetta (2013), Iron fluxes to Talos Dome, Antarctica, over the past 200 kyr, *Clim. Past*, *9*(2), 597–604.
Velicogna, I., and J. Wahr (2013), Time-variable gravity observations of ice sheet mass balance: Precision and limitations of the GRACE satellite data, *Geophys. Res. Lett.*, *40*(12), 3055–3063, doi:10.1002/grl.50527.
Vitousek, P. M., and H. Farrington (1997), Nutrient limitation and soil development: Experimental test of a biogeochemical theory, *Biogeochemistry*, *37*(1), 63–75.
Vitousek, P. M., S. Porder, B. Z. Houlton, and O. A. Chadwick (2010), Terrestrial phosphorus limitation: Mechanisms, implications, and nitrogen-phosphorus interactions, *Ecol. Appl.*, *20*(1), 5–15.
Wolff, E. W., J. C. Moore, H. B. Clausen, and C. U. Hammer (1997), Climatic implications of background acidity and other chemistry derived from electrical studies of the Greenland ice core project ice core, *J. Geophys. Res.*, *102*(C12), 26,325–26,332.
Zamora, L., J. Prospero, D. Hansell, and J. Trapp (2013), Atmospheric P deposition to the subtropical North Atlantic: Sources, properties, and relationship to N deposition, *J. Geophys. Res. Atmos.*, *118*, 1546–1562, doi:10.1002/jgrd.50187.
Zhang, J., P. Wang, Q. Li, X. Cheng, H. Jin, and S. Zhang (2007), Western equatorial Pacific productivity and carbonate dissolution over the last 550 kyr: Foraminiferal and nannofossil evidence from ODP hole 807a, *Mar. Micropaleontol.*, *64*(3), 121–140.
Ziegler, C. L., R. W. Murray, T. Plank, and S. R. Hemming (2008), Sources of Fe to the equatorial Pacific ocean from the Holocene to Miocene, *Earth Planet. Sci. Lett.*, *270*(3), 258–270.
Zielinski, G., P. A. Mayewski, L. Meeker, S. Whitlow, M. Twickler, and K. Taylor (1996), Potential atmospheric impact of the Toba mega-eruption 71,000 years ago, *Geophys. Res. Lett.*, *23*(8), 837–840.